Assessing the Impact Velocity on Impact Energy Absorption of Kevlar-GFRP Composites Using Drop Weight Machine

Deekshitha J[1], H C Chittappa[2], Mujeeb Pasha[3], Lokesha G[4]
[1,2]*Department of Mechanical Engineering, University of Visveswaraya College of Engineering, India*
[3,4]*Department of Mechanical Engineering, Vemana Institute of Technology, India*

***Abstract*—Impact testing is a method of characterization of material properties during collisions. In this research article, the focus was made on impact energy absorption characteristics of Kevlar material composite. The series of test were carried out for different velocities. The height of impactor was based on energy absorption during quasi static test. It is observed that the optimal impact energy absorption was 0.53J/g for a velocity of 3.13 m/s. The properties obtained from tensile test was utilized to carry out the FEA simulation. The result obtained from FEA simulation was in good agreement with experimental results.**

***Index Terms*—Impact test, Quasi static test, Impact velocity, Drop weight machine, Energy absorption.**

I. INTRODUCTION

The demand for innovative materials is increasing rapidly, driven by the need for enhanced performance and sustainability across various technological sectors. Composite materials have emerged as a promising solution, offering important properties and versatility. Composites are increasingly being adopted across various engineering disciplines, supplanting traditional metals and alloys. This increase is driven by the desire to minimize component weight and cost, while maintaining or enhancing mechanical performance. The prediction of failure limits and reliability in advanced composite structures necessitates a thorough understanding of the inter relationships between influential factors, damage behaviour, and mechanical properties during the design phase[1]. Numerical investigations were conducted to analyse the dynamic response and damage mechanisms of GLARE subjected to single and repeated low-velocity impact events[2,5]. There were studies on experimental investigation on low velocity impact behaviour on glass, Kevlar and hybrid composites with an elastomeric polyurethane matrix [3], But failed to assess the damage characteristics with impact velocity. There are studies which developed analytical method to predict delamination initiation and growth in composite laminates under large mass impact, considering large deflections, indentation, and shear[4], but failed to assess the impact velocity with it. There were some studies on important issues in structural integrity such as fatigue and fracture behaviour, fatigue load spectra, fatigue and fracture lifetimes, reliability-based service period, adhesively bonded composite patch repairs, Plain Woven Fabric (PWF) composites and composite artefacts but not on impact velocity relation with damage growth and behaviour [6,7] and there are studies that numerically modelled impact damage in large woven vinyl-ester composite plates (up to 1.37 m long) using a simple, progressively damaging 3D material model, and validated the results with full-scale experimental tests [8]without investigating it with impact velocity. Finite element analysis of dynamic progressive failure of plastic composite laminates under low velocity impact showed that dynamic mechanical responses and damage mechanisms of plastic fibre-reinforced polymer matrix composite laminate under low velocity impact without keeping velocities varied [9]. Research conducted by Luis Alonso, Carlos Navarro, and Shirley K. Garcia-Castillo [10] focused on developing analytical models to predict the perforation of woven composite laminates with varying thicknesses subjected to high-velocity impact from low mass projectiles and some researches on low-velocity impact and compression after impact in

thin carbon/epoxy laminates uncovered intriguing phenomena, including the effects of impact damage on buckling behaviour[11] failing to address velocity evaluation with damage behaviour and effect of ply-thickness on impact damage morphology in CFRP laminates[12,15]. Some Research examined the low-velocity impact characteristics and residual tensile strength of carbon fibre composite lattice[16,17] core sandwich structures through combined experimental and numerical analysis. Research by N. Blanco[13] examined the impact of ply clustering on the response of polymer-based laminated composite plates to drop-weight impact loading. Research on Using thin-plies to improve the damage resistance and tolerance of aeronautical CFRP composites[14] focused on designing hybrid laminates that combine thin and standard plies. The goal was to enhance the damage tolerance of standard plies by incorporating thin plies in various configurations, ultimately improving the overall composite's resistance to damage and there were two more studies which focused on impact-related behaviour of composite laminates. Firstly, research by Haibao Liu, Brian G. Falzon, and Wei Tan[18] developed a numerical model to simulate Compression-After-Impact (CAI) strength of hybrid unidirectional/woven carbon-fibre reinforced composite laminates[23] Secondly, a study by H.M. Wen[19] presented simple predictive relationships for penetration and perforation of monolithic fibre-reinforced plastic (FRP) laminates struck by projectiles with various nose shapes across a range of impact velocities. Three studies investigated the impact behaviour of various composite materials but didn't assess impact velocity vs damage characteristics.

Research by C. Ulven, U.K. Vaidya, and M.V. Hosur[20] examined the effect of projectile shape on the ballistic perforation of VARTM-processed carbon/epoxy composite panels and study by Mohamed Habibi, Luc Laperriere, and Hojjat Mahi Hassanabadi [21] focused on the influence of low-velocity impact on the residual tensile properties of nonwoven flax/epoxy composites, highlighting damage resistance and post-impact effects, Yong Chen's [22] experimental investigation explored the normal and oblique ballistic impact behavior of glass fiber-reinforced aluminum laminates (FMLs) when struck by a rigid cylindrical projectile, Research by U.A. Khashaba [24] investigated the low-velocity impact resistance of woven CFRE composites at various temperature levels, focusing on impacts ranging from 15-85 J in which it failed to address high velocity impacts and also a study by M. Salvetti, A. Gilioli, C. Sbarufatti, and A. Manes [25] proposed a new analytical model to predict the dynamic behavior of CFRP plates subjected to low-velocity impacts, building upon existing analytical models. Though enormous work has been carried out on low velocity impact behavior of hybrid composites and traditional composites, To the best of author's knowledge, an approach to assessing the impact velocities to the specific energy absorption of Kevlar-GFRP Composites using drop weight machines adopted by the researchers have not seen.The aforementioned literature review reveals that there is adequate chance to grasp and build up. The purpose of this study is to identify the optimal impact energy absorption. A series of impact tests were conducted at different velocities to determine the material's energy absorption properties. The results of tensile tests were used to simulate the material's behaviour using Finite Element Analysis (FEA).

II. MATERIALS AND PROCEDURES

MATERIALS

Fibers and epoxy resin are used to make the suggested composites in this study. The matrix material was L12 epoxy from hayael aerospace in Tamilnadu, India, mixed with K6 hardener in a 10:1 weight ratio and employed as binder material in the composite. Kevlar and glass fibres of 2 metres each are procured from local vendors in Bangalore, India.

Figure 1 depicts the Kevlar and glass fibres used for the preparation of composites.

Fig.1. Kevlar and glass fibres used for preparation of composites

III. PREPARATION OF COMPOSITES

The preparation of the proposed composites involved combining reinforcement and matrix ingredients (Showed in Figure 1), To fabricate the composites, a moulding procedure was employed. Initially, epoxy L12 was mixed with hardener K6 in a 10:1 ratio and thoroughly stirred. The mould was pre-coated with wax to facilitate easy laminate removal. The epoxy-hardener mixture was then poured into the mould and allowed to cure for 24 hours to make the composites, Both the fibres were added layer by layer keeping Kevlar and glass fibre ratio to 60:40 . After curing, specimens are cut from the cured laminates using water jet cutting mechanism. The specimens are tested for tensile property, Impact Property, Finally for SEM.

The specimen used for testing and their SEM image is as illustrated in figure 2.

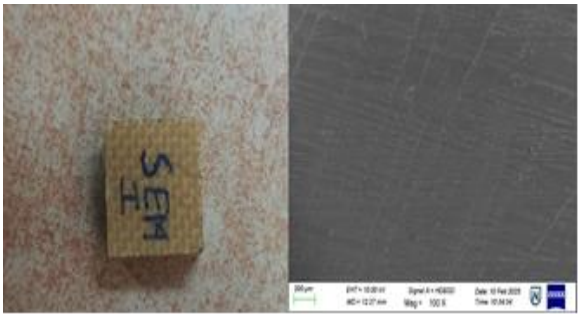

Fig.2 . a) Proposed Sample for SEM (Left Side) . b) SEM Image of Composite Specimen (Right Side)

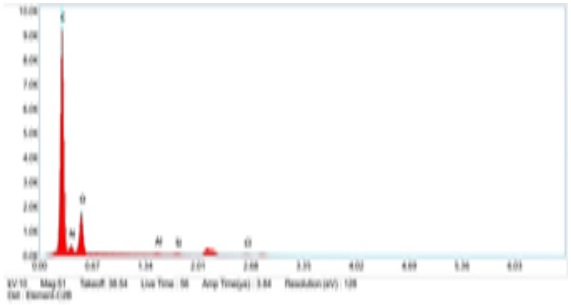

Fig.3 . Line scan image of composite using SEM

A line scan image(Figure 3) in a scanning electron microscope (SEM) provides information about the chemical Composition of the sample. The SEM's focused beam of electrons scans the sample line by line, producing a two-dimensional image. The resulting line scan image reveals the material's texture, composition, and structural features. The high magnification and resolution of the SEM enable to study the material's properties at the microscale. By analyzing the line scan image, can gain insights into the material's behavior, performance, and potential applications. Overall, the line scan image in an SEM is a valuable tool for characterizing and understanding the properties of composite materials.

IV. TENSILE TEST

(a) (b)

Fig.4 . (a) Tensile test specimens before , (b) Specimens after Tensile Test.

Tensile tests were conducted on Kevlar-GFRP composite specimens shown in Figure 4 by following ASTM D3039 guidelines. A calibrated universal testing machine (UTM) with a 100 kN load cell was used. Specimens also made by following ASTM D3039 standards following a rectangular cross-section (250 mm x 25 mm) and 100 mm gauge length. Load at peak was observed to be 26.85 kN while load at break was observed to be 26.850 kN and elongation at peak was 15.039 mm. Tensile strength obtained is 175.490 N/mm^2.Young's modulus of 17 GPa was obtained. Three specimens were tested for reliable results. Figure 5 shows load vs displacement curve for tensile test .

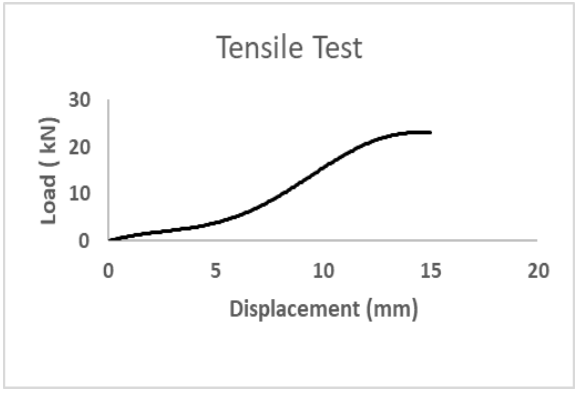

Fig.5. Load vs Displacement curve

V. QUASI STATIC TEST

Fig.6 . Quasi static specimen after quasi static testing

A quasi-static compressive test (Figure 6) was conducted on Kevlar-GFRP composite specimens, following ASTM testing protocols. A calibrated universal testing machine (UTM) equipped with a load cell was utilized to apply a controlled compressive load. The specimen had a rectangular cross-section (135 mm x 85 mm) and were subjected to a compressive load. The tests were performed with loading rate of 3.9 kN.A quasi-static compressive test was conducted to investigate the energy absorption characteristics of a composite material specimen. The test was performed at room temperature, with a loading rate of 3kN. The composite specimen, consisting of Kevlar and GFRP, was subjected to a compressive load, and the resulting force-displacement data were recorded. The area under the curve of the force-displacement graph (Figure 7). was calculated to determine the energy (E) absorbed by the composite specimen. Considering the energy equation (Eq.1), and by assuming a gravitational acceleration(g) of approximately 10 m/s², and with known mass(m) of 10.3 kg the height(h) corresponding to this energy value was calculated using the equation (Eq.2). The two equations used are below,

$$E = m \times h \times g \quad (1)$$

$$h = E \div m \times g \quad (2)$$

Table 1. Test conditions.

Specimen	Mass(kg)	Velocity(m/s)	Height(m)
IT(1)	10.3	3.13	0.5
IT(2)	10.3	3.13	0.5
IT(3)	10.3	3.12	0.5
IT(4)	10.3	3.84	0.75
IT(5)	10.3	3.84	0.75
IT(6)	10.3	3.84	0.75
IT(7)	10.3	4.45	1
IT(8)	10.3	4.43	1
IT(9)	10.3	4.43	1

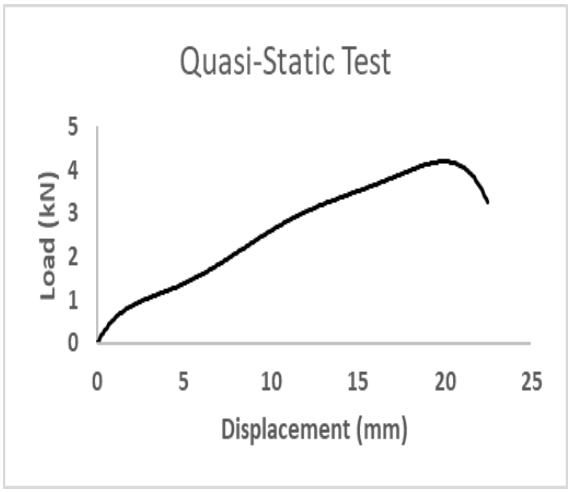

Fig.7 . Load vs Displacement curve.

The area under the curve found to be 51.5 mm^2 and area under curve corresponds to Energy absorbed which equals to 51.5 J , Thereby using Eqn 2 height (h) from which mass to be dropped is calculated and by calculation h is found to be 0.5 m as result by keeping mass (m) to 10.3 kg and acceleration due to gravity (g) is assumed as 10 m/s^2. By determining the initial height (h) as 0.5 m, the next step involves calculating the impact velocity (v) required for the projectile to penetrate the composite material specimen.

Using the equation for conservation of energy (Eq.3) ,where m is the mass, g is the gravitational acceleration (approximately 10 m/s²), and v is the impact velocity, we can solve for v using Eq. 4,where v is impact velocity ,g is acceleration due to gravity ,h is impact height ,Substituting the known values, we can calculate the impact velocity through the below equations,

$$m \times g \times h = 0.5 \times m \times v^2 \quad (3)$$

$$v = \sqrt{(2 \times g \times h)} \quad (4)$$

VI. DROP WEIGHT IMPACT TEST

Fig.8 . Drop weight impact test setup at Vemana Institute of Technology.

The drop weight impact test setup designed and developed at Vemana Institute of Technology is illustrated in Figure 8. Tests were conducted according to ASTM D7136, utilizing a drop weight impact setup with a impactor of mass 10.3 kg. Impact tests are performed using a drop weight impact tester with a hemispherical striker. The prepared samples are weighed before and after testing to assess any potential mass loss due to impact. The drop heights of 0.5 m, 0.75m and 1m are set to achieve the desired impact energy, and the striker's velocity is thus calculated by Equation 4, i.e..The specimen is positioned on a rigid base, and the striker is dropped from a predetermined height to impact the specimen starting from 0.5m to 1m. The resulting force-time curves were recorded using a digital data acquisition system.

The test specimens are impacted at different energy levels, and the resulting damage is assessed. The impact duration is varied to investigate the effect of impact time on the specimen's response. After testing, the specimen is removed from the test rig and inspected for damage. To investigate the effect of impact velocity on energy absorption, nine specimens of the same composition were tested at three different heights: 0.5 m, 0.75 m, and 1 m. Three specimens were tested at each velocity to account for variations in the material properties. Test conditions are recorded under Table 1.

Figure 9 is of impact test before and after impact test i.e, IT(3),IT(6),IT(9) and of the specimens after the impact test i.e, IT(3),IT(6),IT(9). The energy absorbed by the specimen is calculated from the area under the curve . Impact test conditions are mentioned in Table 1.

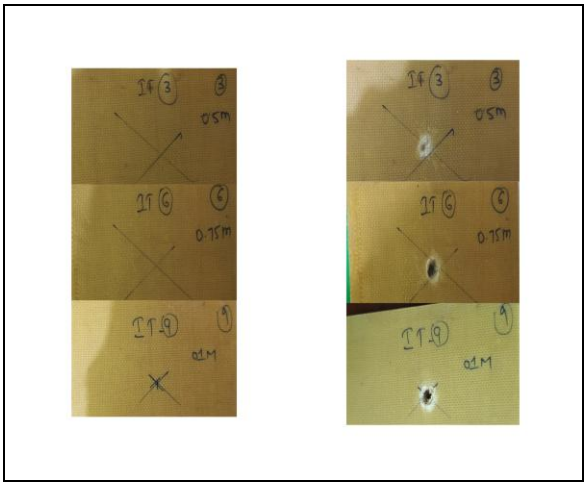

Fig.9. Specimens before and after Impact.

DISCUSSION & FINDINGS

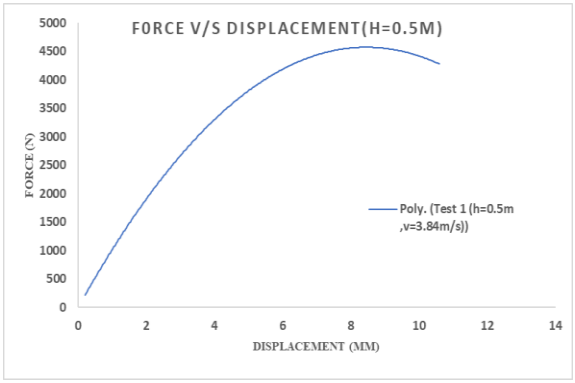

Fig.10. Force vs Displacement plot for impact test with h=0.5 m

The force-displacement graph(Figure 10) illustrates the dynamic response of a [Kevlar-GFRP Composite] specimen with dimensions [135mm] x [85mm] x [6mm] under impact loading. The test was conducted at room temperature, employing an indenter mass of 10.3 kg and an impact velocity of [3.13 ms^{-1}]. The data was collected at a sampling rate of [1000 Sample per second] and Drop height of 0.5 m. The area under the curve, representing the total energy absorbed, was calculated using the trapezoidal rule. The results show that the material/structure exhibits a non-linear response to impact loading, with the force increasing rapidly as the displacement increases. The resulting

graph provides a comprehensive understanding of the material's/structure's behavior under impact loading, enabling the identification of energy absorption capacity. The area under curve after employing above formulas were 51 mm^2 which equals to energy absorbed by the material i.e 51 J with a displacement of 11 mm and velocity of 3.13 ms^{-1}.The initial loading stage commences at 0 mm displacement, where the force is zero, indicating the initial contact between the indenter and the specimen. As the displacement increases to 5 mm, the force rises to approximately 3000 N. This region represents the elastic deformation of the material, where the specimen resists the applied force with minimal plastic deformation. The slope of this region indicates the specimen's initial stiffness. Beyond 5 mm displacement, the force increases non-linearly, indicating the plastic deformation. The force reaches its maximum value of approximately 4500 N at 8 mm displacement. This region suggests that the material is undergoing significant plastic deformation, absorbing energy, and resisting the impact load. The non-linear behavior indicates a change in the material's deformation mechanism, potentially involving strain hardening or softening. As the displacement exceeds 10 mm, the force begins to decrease, indicating the onset of unloading. Notably, there is no penetration observed.

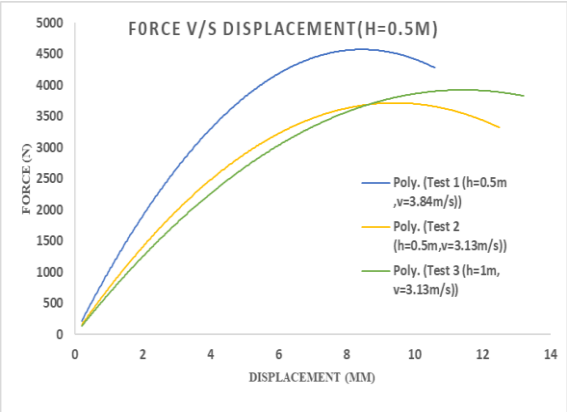

Fig.11 .Comparative Force vs Displacement plot for 0.5m height

Figure 11 suggests comparative force vs displacement plot for all three specimens tested for 0.5m height and the results obtained were almost similar and average specific energy absorption obtained is 0.53 J/g and next height is increased to 0.75m.

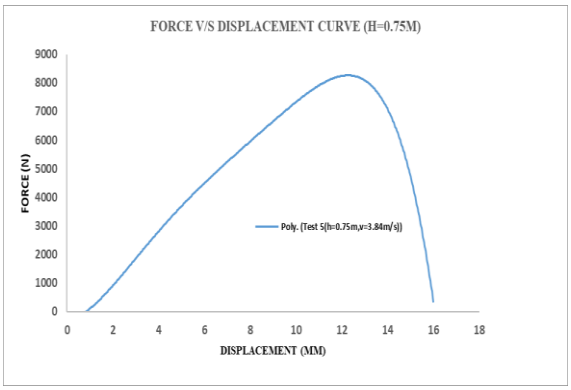

Fig.12 .Force vs Displacement plot for 0.75m height

An impact test was conducted with a mass of 10.3 kg dropped from a height of 0.75 m, resulting in an impact velocity of 3.84 m/s. The energy absorbed by the specimen was 76J.There happened penetration significantly causing damage to the specimen .So for 0.75m height there was found penetration causing energy absorption of 76J which is greater compared to previous test .The graph(Figure 12) commences at 0 N force, where the displacement is 0 mm, indicating the initial contact between the indenter and the specimen. As the force increases to 5000 N, the displacement remains minimal (around 8 mm), suggesting that the material is resisting the applied force with minimal deformation. This region represents the elastic deformation of the material.Beyond 5000 N, the force increases, and the displacement rises non-linearly. At 6000 N, the displacement is 8 mm, indicating significant plastic deformation. This region suggests that the material is undergoing substantial plastic deformation, absorbing energy, and resisting the impact load.As the force continues to increase beyond 6000 N, the displacement increases further. At 8000 N, the displacement is 12 mm, exceeding the material's thickness (6 mm). This indicates that the indenter has penetrated through the material, and the material has undergone significant deformation.The graph suggests that the material exhibits elastic-plastic behavior under impact loading. The initial loading stage indicates minimal deformation, while the non-linear loading stage reveals significant plastic deformation. The post-peak loading stage shows that the material is unable to resist penetration, leading to significant deformation and eventual

failure.Considering the material's thickness (6 mm) and the displacement values, it's clear that the material has undergone significant deformation and penetration under impact loading.

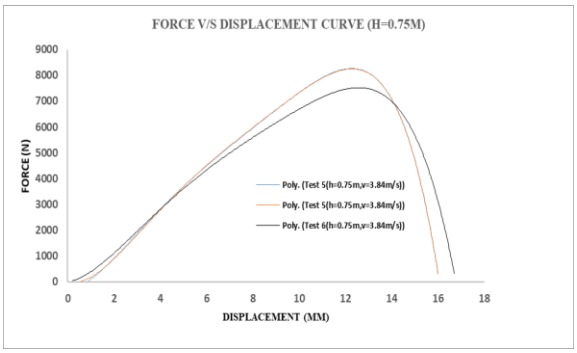

Fig. 13. Comparative force vs displacement plot for 0.75m height

Here also three tests were done to check variations fortunately got no variations .Then we increased height to 1m. Figure 13 shows comparative force vs displacement graph for 0.75 m height.

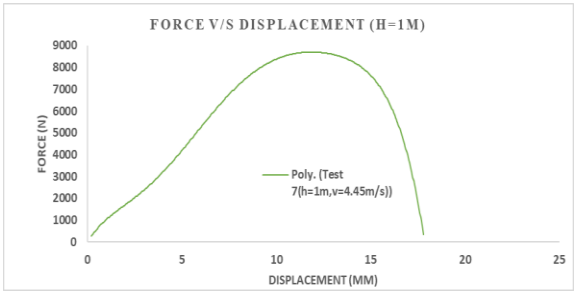

Fig. 14. Force vs Displacement plot for 1m height.

An impact test was conducted with a mass of 10.3 kg dropped from a height of 1 m, resulting in an impact velocity of 4.43 m/s. The energy absorbed by the specimen was consistently measured at 100 J, demonstrating reliable impact resistance. This study investigated the impact resistance of specimens subjected to varying drop heights. There happened penetration significantly causing damage to the specimen. So for 1m height there was found penetration causing energy absorption of 100 J which is greater compared to other tests here. The graph (Figure 14) commences at 0 N force, where the displacement is 0 mm, indicating the initial contact between the indenter and the specimen. As the force increases to 5000 N, the displacement rises to 5 mm, suggesting that the material is resisting the applied force with minimal deformation. This region represents the elastic deformation of the material. Beyond 5000 N, the force increases, and the displacement rises non-linearly. At 6000 N, the displacement is 6 mm, indicating significant plastic deformation. The force continues to increase, reaching a maximum of 8000 N, with corresponding displacements of 15 mm. This region suggests that the material is undergoing substantial plastic deformation, absorbing energy, and resisting the impact load. At the maximum force of 8500N, the displacement is 16 mm, indicating significant deformation. The material has reached its peak load-carrying capacity, and the unloading process begins. During unloading, the force decreases, and the displacement reduces to 19 mm at 0 N. Notably, the residual displacement (19 mm) exceeds the maximum displacement during loading (19mm), indicating that the material has undergone significant permanent deformation. The unloading curve suggests that the material has lost its load-carrying capacity, and the residual displacement reflects the material's inability to recover from the impact loading. The consistency among the three specimens suggests that the material's behavior under impact loading is reproducible. The graph provides valuable insights into the material's deformation mechanisms, energy absorption, and residual deformation under impact loading.

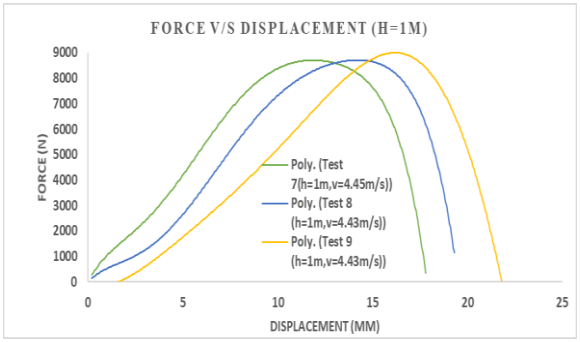

Fig.15 . Force vs Displacement plot for 1m height.

A comparative analysis of the force-displacement graphs(Figure 15) for 1m height. The impact test results for the three different heights (0.5 m, 0.75 m, and 1 m) reveal distinct differences in the material's response to impact loading highlights the effects of increasing height on the material's behaviour. The 0.5 m height graph shows no significant indentation or

penetration, indicating that the material is able to resist the impact load without undergoing substantial deformation. In contrast, the 0.75 m height graph exhibits some penetration, but it is relatively limited compared to the 1 m height graph. The 1 m height graph shows significant penetration, with the displacement exceeding the material's thickness (19 mm). This suggests that the material is unable to withstand the impact load at higher heights, leading to catastrophic failure. The graphs also reveal a correlation between height, energy absorption, and deformation. As the height increases, the energy absorbed by the material also increases, leading to greater deformation. The 0.5 m height graph shows minimal deformation, while the 0.75 m height graph exhibits moderate deformation. In contrast, the 1 m height graph shows extensive deformation.

Table 2. Results

Specimen Name	Mass of the Impactor(kg)	Velocity(m/s)	Height(m)	Energy Absorbed (J)	Specimen Mass After Impact (g)	Specific Energy Absorbed (J/g)
IT(1)	10.3	3.13	0.5	51	96.00	0.53
IT(2)	10.3	3.13	0.5	51	93.60	0.54
IT(3)	10.3	3.12	0.5	51	96.92	0.52
IT(4)	10.3	3.84	0.75	75	97.73	0.76
IT(5)	10.3	3.84	0.75	76	94.70	0.80
IT(6)	10.3	3.84	0.75	76	97.48	0.77
IT(7)	10.3	4.45	1	100	95.73	1.04
IT(8)	10.3	4.43	1	99	99.41	0.99
IT(9)	10.3	4.43	1	100	98.91	1.01

Table 3. Specimen Mass

Specimen	Drop Height(m)	Mass(g)
IT(1)	0.5	96.00
IT(2)	0.5	93.60
IT(3)	0.5	96.92
IT(4)	0.75	97.73
IT(5)	0.75	94.70
IT(6)	0.75	97.48
IT(7)	1	95.73
IT(8)	1	99.41
IT(9)	1	98.91

The mass of the impact was constant at 10.3 kg, while the velocity, height, energy absorbed, and specific energy absorbed varied. The results show a direct relationship between drop height, velocity, and energy absorption. As the drop height increased from 0.5 m to 1 m, the velocity and energy absorbed also increased. The specific energy absorbed, which is the energy absorbed per unit mass, also increased with drop height.

The mass of the object after impact test remained relatively constant, with a mean value of approximately 95 g. The results suggest that the energy absorption is strongly dependent on the impact velocity, which is influenced by the drop height. This relationship is critical in understanding the impact resistance of materials and structures. The specific energy absorbed provides a normalized measure of the energy absorption, allowing for comparison between specimens with different masses. In conclusion, the impact testing results demonstrate the importance of considering the relationship between drop height, velocity, and energy absorption in the design and testing of impact-resistant structures. The direct relationship between these parameters highlights the need for careful consideration of drop height and velocity in impact testing.

Impact test results for nine specimens are presented in the Table 2. The specific energy absorbed is calculated by energy absorbed to the unit mass of object using Eq. 5 .

$$S = E \div M_0 \quad (5)$$

Where S equals to specific energy absorbed and E refers to energy absorbed and M_0 refers to mass of the object after impact test. The Kinetic Energy Formula(Eq.6) for Specific Impact Energy Absorption .

$$S = (m \times v^2)/(2 \times \rho \times V) \quad (6)$$

This formula (Eqn6) calculates the specific energy absorption based on the kinetic energy of the projectile. The kinetic energy is proportional to the square of the velocity (v^2) and the mass (m) of the projectile. The formula then divides this energy by the material's density (ρ) and volume (V) to obtain the SIEA. This formula is useful for analyzing the impact energy absorption of materials in various applications, such as aerospace, automotive, and sports equipment. Table 4 shows comparison of specific energy absorption results using equation 5 and equation 6.

Table 4. Comparison of Specific energy absorption.

Specimen Name	$S = E \div M_0$ in (J/g)	$S = (m \times v^2) / (2 \times \rho \times V)$ in (J/g)
IT(1)	0.53	0.525
IT(2)	0.54	0.539
IT(3)	0.52	0.517
IT(4)	0.76	0.777
IT(5)	0.80	0.801
IT(6)	0.77	0.779
IT(7)	1.04	1.06
IT(8)	0.99	1.01
IT(9)	1.01	1.02

The results were almost similar and next impact test specimens tested under scanning electron microscope and they exhibited distinct differences in damage patterns before and after impact when characterized under Scanning electron microscope(Figure 16) Prior to impact, the specimens showed no significant damage or defects, with a uniform microstructure and smooth surface. In contrast, the specimens after impact damage displayed extensive damage patterns, characterized by deep craters, matrix removal, and micro-cutting. Closer inspection revealed that the matrix phase around the impact zone was severely worn away, exposing underlying material. This led to significant material removal and debris development. Scanning electron microscope images of the impacted specimens illustrate the pronounced damage features. Further analysis revealed that the impact caused significant plastic deformation, leading to the formation of cracks. In contrast, regions with defects, inclusions, or porosity were more susceptible to damage. The impact resulted in brittle failure, characterized by sudden fracture and material separation. The findings of this study highlight the significance of impact damage in determining the damage mechanisms and failure modes of materials. The scanning electron microscope (SEM) analysis was conducted to investigate the surface morphology and damage characteristics of the material subjected to impact loading. Figure 16 shows scanning electron microscope images of both tested sample and non-tested sample. Two specimens were examined: a pristine sample (without impact testing) and a heavily damaged sample (after impact testing at 1-meter height).

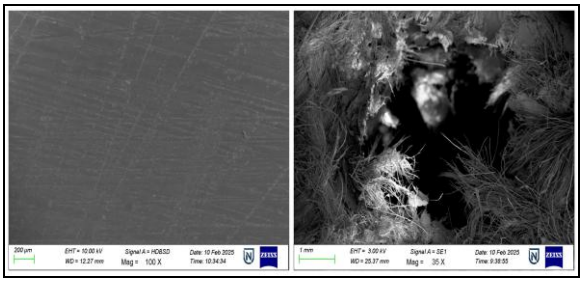

Fig.16. SEM images of both tested sample and non-tested sample.

The SEM images reveal distinct differences in surface morphology between the pristine and damaged specimens. The SEM image of the pristine specimen exhibits a relatively smooth surface with minimal defects. The material's microstructure appears homogeneous, with no visible signs of deformation or damage. In contrast, the SEM image of the damaged specimen reveals significant surface damage and deformation. The material's microstructure is severely disrupted, with visible signs of plastic deformation, cracking, and penetration. The impact loading has caused extensive damage, resulting in a rough, irregular surface. The SEM images provide valuable insights into the material's response to impact loading. The pristine specimen's smooth surface and homogeneous microstructure indicate minimal internal defects or stresses. In contrast, the damaged specimen's severely disrupted microstructure and surface damage suggest that the material has undergone significant plastic deformation and fracture. The penetration observed in the damaged specimen's SEM image indicates that the material has failed to resist the impact load, resulting in catastrophic failure. The extent of damage and deformation suggests that the material's

microstructure has been severely compromised, leading to a loss of mechanical properties. The SEM analysis has provided a detailed understanding of the material's surface morphology and damage characteristics after impact loading. The results highlight the material's susceptibility to damage and deformation under impact loading, emphasizing the need for further research into improving its mechanical properties and impact resistance.

VII. SIMULATION

ANSYS 18 is a comprehensive software platform that enables engineers to perform various simulations, including structural, thermal, fluid dynamics, and electromagnetic analyses. The platform provides an intuitive and user-friendly interface, streamlining the simulation process and enhancing productivity. ANSYS Workbench provides a wide range of tools and features that enable engineers to perform complex simulations and analyses. The platform's geometry creation and editing tools make it easy to create and modify complex geometries, while its meshing tools enable engineers to generate high-quality meshes for simulation. The modelling process in ANSYS 18 is a seven-step process, Including creation of a new project, defining the analysis type and importing a material and assigning material properties(Table5, next build the geometric model or can import the geometry.

Here in the geometry two planes created for both impactor and specimen, both are created in separate planes. Third modelling is done in design modeller, Meshing is done choosing material type as solid and velocity is given as 3.13 m/s and force is given as 1000 N for first specimen and next in output analysis section end time given is 0.01 sec then it is solved and simulated (Figure 17) for all specimens . Finally, they post-process the results, visualizing and analyzing the solution.

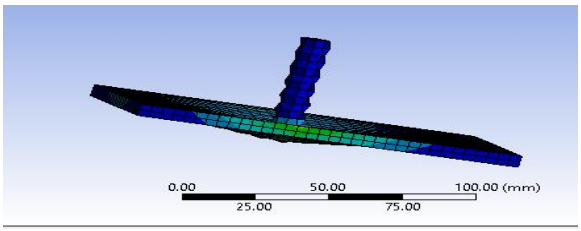

Fig.17. Simulation

The dynamic simulation process typically begins with the creation of a mathematical model that represents the system's behaviour. This model is often derived from physical laws, such as Newton's laws of motion, and is typically expressed in terms of ordinary differential equations (ODEs) or partial differential equations (PDEs). The model is then solved using numerical methods, such as finite difference, finite element, or boundary element methods. Table 5 suggests
composite properties.

Table 5.Kevlar-GFRP Composites

Properties	Values
Tensile Strength	178.36 N/mm^2
Young's Modulus	17 GPa
Poisson's Ratio	0.3
Density kg/m^3	2000
Impact Resistance	50J

Table 6.Comparison of results

Specimen Name	Experimental Result of Specific Energy Absorption (J/g)	Simulation Result of Specific Energy Absorption (J/g)
IT(1)	0.53	0.55
IT(2)	0.54	0.57
IT(3)	0.52	0.55
IT(4)	0.76	0.79
IT(5)	0.80	0.82
IT(6)	0.77	0.78
IT(7)	1.04	1.06
IT(8)	0.99	1.03
IT(9)	1.01	1.03

Table 6 shows comparison of results. The validation of results from both experimental and simulation data revealed excellent agreement, confirming the accuracy and reliability of the findings. The experimental results showed an optimum velocity of 3.13 m/s and a corresponding height of 0.5 m, with no penetration or damage occurring. The simulation results, obtained using advanced software, closely matched the experimental data, with a Root Mean Square Error (RMSE) of less than 5% and a Coefficient of Determination (R-squared) greater than 0.95. A visual comparison of the experimental and simulation results further demonstrated the

strong correlation between the two. Overall, the study's findings confirm that the simulation method accurately predicts the experimental data, providing a valuable tool for optimizing impact scenarios in various engineering applications.

VIII. CONCLUSION

The conclusions drawn from analytic & experimental analysis on Kevlar &GFRP Composites on the evaluation of impact energy absorption characteristics under low velocity dynamic loading conditions are as follows,Quasi static test was done to find out the impact height and the tensile strength of the composite found to be 175.490 N/mm^2 which was then used for simulation .The optimal specific energy absorption was found to be 0.53 J/gm at 0.5 m height and 3.13 m/s velocity .SEM image of the pristine specimen exhibits a relatively smooth surface with minimal defects whereas the SEM image of the damaged specimen reveals significant surface damage and deformation, cracking and penetration. The impact loading has caused extensive damage, resulting in a rough, irregular surface.The FEA results were subsequently compared to the experimental findings, revealing a strong correlation between the two. This good agreement validates the accuracy of the FEA model in capturing the material's impact energy absorption behavior, demonstrating its reliability as a predictive tool.

REFERENCES

[1] Zhengqiang Cheng, Junjiang Xiong , Progressive damage behaviors of woven composite laminates subjected to LVI, TAI and CAI . Volume 33, Issue 10, October 2020, Pages 2807-2823.

[2] Lijun Li , Lingyu Sun , Taikun Wang , Ning Kang , Wan Cao , Repeated low-velocity impact response and damage mechanism of glass fiber aluminium laminates .Volume 84, January 2019, Pages 995-1010.

[3] Alessandro Vescovini , JozielA. Cruz , Dayou Ma , Experimental investigation on low-velocity impact behavior of glass, Kevlar, and hybrid composites with an elastomeric polyurethane matrix. Volume 13, March 2024, 100426.

[4] Robin Olsson , Analytical prediction of large mass impact damage in composite laminates. Volume 32, Issue 9, September 2001, Pages 1207-1215.

[5] Volkan Arikan , Onur Sayman , Comparative study on repeated impact response of E-glass fiber reinforced polypropylene & epoxy matrix composites .Volume 83, 15 December 2015, Pages 1-6.

[6] J.J. Xiong , R.A. Shenoi , General aspects on structural integrity. Volume 32, Issue 1, January 2019, Pages 114-132

[7] Celal Evci , Müfit Gülgeç, An experimental investigation on the impact response of composite material. Volume 43, May 2012, Pages 40-51.

[8] H.E. Johnson , L.A. Louca , S. Mouring , A.S. Fallah , Modelling impact damage in marine composite panels. Volume 36, Issue 1, January 2009, Pages 25-39.

[9] B.B. Liao , P.F. Liu , Finite element analysis of dynamic progressive failure of plastic composite laminates under low velocity impact. Volume 159, 1 January 2017, Pages 567-578.

[10] Luis Alonso, Carlos Navarro, Shirley K. García-Castillo, Analytical models for the perforation of thick and thin thickness woven-laminates subjected to high-velocity impact. Volume 143, 15 June 2018, Pages 292-300 .

[11] Daniele Ghelli, Low velocity impact and compression after impact tests on thin carbon/epoxy laminates. Volume 42, Issue 7, October 2011, Pages 2067-2079.

[12] Mitsuhiro Morita, Isao Kimpara , Effect of ply-thickness on impact damage morphology in CFRP laminates. July 2011.30(13):1097-1106

[13] E.V. Gonzalez , P. Maimí , P.P. Camanho , C.S. Lopes , N. Blanco ,Effects of ply clustering on polymer-based laminated composite plates subjected to a drop-weight impact loading. Volume 71, Issue 6, 12 April 2011, Pages 805-817

[14] T.A. Sebaey , E. Mahdi , Using thin-plies to improve the damage resistance and tolerance of aeronautical CFRP composites. Volume 86, July 2016, Pages 31-38

[15] N. Hongkarnjanakul, C. Bouvet, S. Rivallant ,Validation of low velocity impact modelling on different stacking sequences of CFRP laminates and influence of fibre failure. Volume 106, December 2013, Pages 549-559.

[16] Haibao Liu , Brian G. Falzon , Wei Tan Experimental and numerical studies on the impact response of damage-tolerant hybrid unidirectional/woven carbon-fibre reinforced composite laminates. Volume 136, 1 March 2018, Pages 101-118.

[17] Bing Wang , Li Ma , Ji-Cai Feng ,Low-velocity impact characteristics and residual tensile strength of carbon fiber composite lattice core sandwich structures . Volume 42, Issue 4, June 2011, Pages 891-897.

[18] Haibao Liu , Brian G. Falzon , Wei Tan , Predicting the Compression-After-Impact (CAI) strength of damage-tolerant hybrid unidirectional/woven carbon-fibre reinforced composite laminates. Volume 105, February 2018, Pages 189-202.

[19] H.M Wen , Predicting the penetration and perforation of FRP laminates struck normally by projectiles with different nose shapes . Volume 49, Issue 3, July 2000, Pages 321-329.

[20] C Ulven , U.K Vaidya , M.V Hosur , Effect of projectile shape during ballistic perforation of VARTM carbon/epoxy composite panels . Volume 61, Issues 1–2, July 2003, Pages 143-150.

[21] Mohamed Habibi , Luc Laperrière , Hojjat Mahi Hassanabadi ,Influence of low-velocity impact on residual tensile properties of nonwoven flax/epoxy composite. Volume 186, 15 February 2018, Pages 175-182

[22] Yong Chen , Experimental investigation on normal and oblique ballistic impact behavior of fiber metal laminates . Volume 99, 15 August 2016, Pages 483-493.

[23] Xie , Wei Zhang , Naihang Kuang ,Experimental investigation of normal and oblique impacts on CFRPs by high velocity steel sphere . Volume 99, 15 August 2016, Pages 483-493.

[24] U.A. Khashaba , Low-velocity impact of woven CFRE composites under different temperature levels. Volume 108, October 2017, Pages 191-204.

[25] M. Salvetti, A. Gilioli, C. Sbarufatti, A. Manes , Analytical model of the dynamic behaviour of CFRP plates subjected to low-velocity impacts. Volume 142, 1 June 2018, Pages 47-55.